

## Solvatochromism, Prototropism and Complexation of *para*-aminobenzoic Acid

T. STALIN<sup>1</sup>, B. SHANTHI<sup>2</sup>, P. VASANTHA RANI<sup>2</sup> and N. RAJENDIRAN<sup>1,\*</sup>

<sup>1</sup>Department of Chemistry, Annamalai University, Annamalainagar, 608 002, Tamil Nadu, India; <sup>2</sup>Department of Physics, Annamalai University, Annamalainagar, 608 002, Tamil Nadu, India

(Received: 15 May 2005; in final form: 12 August 2005)

**Key words:** *p*-Aminobenzoic acid,  $\beta$ -cyclodextrin, inclusion complex, solvent and pH effects

### Abstract

Effect of solvents, buffer solutions of different pH and  $\beta$ -cyclodextrin ( $\beta$ -CD) on the absorption and fluorescence spectra of *p*-aminobenzoic acid (*p*ABA) have been investigated. The inclusion complex of *p*ABA with  $\beta$ -CD is investigated by UV-visible, fluorimetry, semiempirical quantum calculations (AM1), <sup>1</sup>H NMR and Scanning Electron Microscope (SEM). The thermodynamic parameters ( $\Delta H$ ,  $\Delta G$  and  $\Delta S$ ) of the inclusion process are also determined. The experimental results indicated that the inclusion processes is an exothermic and spontaneous. The large Stokes shift emission in solvents with *p*ABA are correlated with different solvent polarity scales. The increase in the excited dipole moment values suggest that *p*ABA molecule is more polar in the S<sub>1</sub> state. Solvent and  $\beta$ -CD studies indicates intramolecular charge transfer in *p*ABA is less than *ortho* and *meta* isomers. Acidity constants for different prototropic equilibria of *p*ABA in the S<sub>0</sub> and S<sub>1</sub> states are calculated.  $\beta$ -Cyclodextrin studies shows that *p*ABA forms a 1:1 inclusion complex with  $\beta$ -CD. A mechanism is proposed to explain the inclusion process.

### Introduction

The spectroscopic properties of *para*-aminobenzoic acid derivatives (*p*ABA) have been studied in the last few years [1–3]. The reason for interest lie in its application as medicinal importance [4]. It has some therapeutic effect against typhus and other ricketisial diseases. In the clinical laboratory, this compound is often used as a sulfonamide antagonist and more commonly it is used as a sunscreen agent [5]. Recently many analytical methods have been developed for the qualification of *p*ABA [6]. In addition, the luminescence characteristics of *p*ABA are of interest based on many solid matrices, such as filter paper [7], polyvinyl alcohol substrate [8], sodium acetate [9], sodium acetate/sodium chloride [10] and CD/NaCl [11]. Especially enhanced fluorescence or phosphorescence emissions are observed on a CD/NaCl solid substrate. The interaction mode of CD/*p*ABA absorbed on a solid matrix is attributed to hydrogen bonding between the carbonyl group in the *p*ABA molecule and the hydroxyl group in cyclodextrin (CD). At present the interaction of CD and *p*ABA is limited to solid matrix systems. It is necessary, therefore to study the inclusion interaction of  $\beta$ -CD with *p*ABA in solution.

In recent years, CDs have received considerable attention. They are interesting microvessels for approximately sized molecules and the resulting supra-

molecules serve as excellent miniature models of enzyme–substrate complexes. CDs with different cavity diameters have been used advantageously to sequester guests on the basis of size, e.g., simple benzene derivatives fit easily within  $\alpha$ -CD, and larger aromatics can be accommodated within  $\beta$ -CD or  $\gamma$ -CD according to their molecular dimensions. The reduced polarity and the restricted space provided by the CD cavity markedly influence a number of photophysical and/or photochemical processes [12]. The formation of a CD inclusion complex means that compatibility is reached between the host and guest in terms of the polarity and stereochemistry [1–3]. On formation of the complex with the guest molecule experiences a non-polar environment and possesses a decreased freedom for bulk and intramolecular rotations in the rigid non-polar CD cavity. The charge transfer character is strongly dependent on the medium polarity and viscosity. Thus, the formation of a CD inclusion complex is expected to have a significant effect on the charge transfer process of the included compound [13]. Further, Shizuka *et al.* [14] have demonstrated that prototropic reactions are affected by inclusion of the substrate molecules in CD cavities.

In the last few years, our main emphasis has been to study the effect of solvents of different polarity, pH and  $\beta$ -cyclodextrin on the spectral characteristics of different fluorophores [15, 16]. Recently 2- and 3-aminobenzoic acids [17] has been studied and this molecules shows

\* Author for correspondence. E-mail: drrajendiran@rediffmail.com

intramolecular charge transfer (ICT) emissions in the excited state. Jiang [1] and Kim *et al.* [3] have reported, 'twisted intramolecular charge transfer' (TICT) behavior of *p*-dimethylaminobenzoic acid and *p*-diethylaminobenzoic acid in  $\alpha$  and  $\beta$ -CD solutions. This stimulated us to carry out to the study the effect of solvents, pH and  $\beta$ -CD on spectral characteristics of *p*-aminobenzoic acid.

## Experimental

Absorption spectral measurements were carried out with a Hitachi Model U-2001 UV-visible spectrophotometer, and fluorescence measurements were made using a Jasco FP-550 spectrofluorimeter. The pH values in the range 2.0–12.0 were measured on Elico pH meter model LI-10T. Microscopic morphological structure measurements were performed with JEOL JSM 5610 LV scanning electron microscope (SEM). Bruker Advance DRX 400 MHz super conducting NMR spectrophotometer was used to study  $^1\text{H}$  NMR spectra.

*p*ABA and  $\beta$ -CD were obtained from E-merck and recrystallized from aqueous ethanol. The purity of the compound was checked by similar fluorescence spectra when excited with different wavelengths. All solvents used were of the highest grade (spectrograde or AnalaR) commercially available. Triply distilled water used for the preparation of aqueous solutions. Solutions in the pH range 2.0–12.0 were prepared by adding the appropriate amount of NaOH and  $\text{H}_3\text{PO}_4$ . A modified Hammett's acidity scale ( $H_0$ ) [18] for the solutions below pH  $\sim 2$  (using a  $\text{H}_2\text{SO}_4$ - $\text{H}_2\text{O}$  mixture) and Yagil's basicity scale ( $H_-$ ) [19] for solutions above pH  $\sim 12$  (using a NaOH- $\text{H}_2\text{O}$  mixture) were employed. The solutions were prepared just before taking measurements. The concentrations of the solutions were of the order  $10^{-4}$  to  $10^{-5}$  mol  $\text{dm}^{-3}$ . All experiments were carried out at 30 °C. The concentration of  $\beta$ -CD was varied from zero to  $1.2 \times 10^{-2}$  mol  $\text{dm}^{-3}$ . The solid inclusion complex was also prepared by coprecipitation method and analysed by  $^1\text{H}$  NMR and SEM methods.

## Results and discussion

### Effect of solvents

The absorption and fluorescence spectra of *p*ABA have been observed in solvents of different polarities and hydrogen bonding abilities. The relevant data are listed in Table 1. In all solvents, the absorption and emission solvatochromic shifts of *o*ABA ( $\lambda_{\text{abs}} - 333, 247$  nm,  $\lambda_{\text{emi}} - 410$  nm) and *m*ABA ( $\lambda_{\text{abs}} - 319, 220$  nm;  $\lambda_{\text{emi}} - 430$  nm) are found to be more than that of *p*ABA ( $\lambda_{\text{abs}} - 283, 217$  nm;  $\lambda_{\text{emi}} - 320$  nm all values in methanol) indicating that, both in the ground and excited states the charge transfer interaction from amino to carbonyl group in *p*ABA is less than *ortho* and *meta* isomers. The

absorption spectrum of *p*ABA in water, at pH  $\sim 7$  is largely blue shifted (265 nm) than other solvents. Acidic pH  $\sim 3.0$ , does not dramatically affect the appearance of the spectrum except for a red shift (282 nm). This effect of the pH on the absorption spectrum indicates that the carboxyl group is ionized in pH  $\sim 7$ , because deprotonation of carboxyl group is blue shifted.

The fluorescence spectra of *p*ABA is constantly red shifted under similar environment. On comparison with *o*ABA and *m*ABA the emission maxima of *p*ABA is largely blue shifted in all solvents. A larger red shift is observed in the  $S_1$  state in *ortho* and *meta* isomers (*o*ABA,  $\lambda_{\text{emi}} - 410$  nm and *m*ABA,  $\lambda_{\text{emi}} - 430$  nm, in methanol) reflects the greater delocalization of the  $\pi$ -cloud of the carboxyl group and lone pair of the amino group with the aromatic moiety. However, in *p*ABA, there is no discernible effect is observed in solvents is explained as follows: of the three aminobenzoic acids the *ortho* and *meta* isomers can undergo a greater ICT character in the  $S_1$  state, whereas *para* isomer can undergo a tautomerism of the amino-imino type [20]. Further intramolecular hydrogen bond and zwitter ions are present in *o*ABA, whereas in *m*ABA, the *meta* directing carbonyl group effectively increases the charge transfer character from the amino group to carbonyl group. Hence a larger red shift is observed in *ortho* and *meta* isomers than *para* isomer.

The bandwidth of *p*ABA is also smaller than other two isomers. The larger blue shift and smaller bandwidth in *p*ABA suggest, ICT (TICT) is not present in *p*ABA. It is further supported, *p*-dimethylaminobenzoic acid does not exhibit the excited state TICT emission in non-polar solvents because of a weak dipole-dipole interaction between solute and solvent and a fast back charge transfer [3]. The geometry of *p*ABA is also optimized using the AM1 method it shows bond angle of amino group is not deviated from  $120^\circ$  is confirmed ICT (TICT) is not present in *p*ABA molecule.

Figure 1 represents the plots of  $\Delta\bar{\nu}_{\text{ss}}$  versus  $E_T(30)$ , BK and  $f(D,n)$  solvent parameters. The correlation of Stokes shifts with Dimroth-Reichardt's [21],  $E_T(30)$ , Bilot-Kawski [22] (BK) and Lippert [23]  $f(D,n)$  values any one of these parameters gives an idea of about the type of interaction between the solute and solvent can be obtained. The increase in Stokes shifts from cyclohexane to water in *p*ABA is found to be more in accordance with  $E_T(30)$  than with BK/ $f(D,n)$  parameters. The solvatochromic shifts reveal that the hydrogen bonding interactions are present along with dipole interactions. In order to confirm this, we used the above solvent parameters and the values are compared with Stokes shifts of *p*ABA molecule (Table 1). Since H-bonding interactions are predominant in the solvatochromic shifts of *p*ABA  $E_T(30)$  parameters gives good correlation ( $r=0.850$ ) than the other two parameters (BK,  $r=0.546$ ;  $f(D,n)$ ,  $r=0.549$ ). Further, the ground state dipole moment ( $\mu_g = 4.51$  D) is also determined by using AM1 method and the excited state dipole moment ( $\mu_e = 7.97$  D) is calculated by using Lippert equation

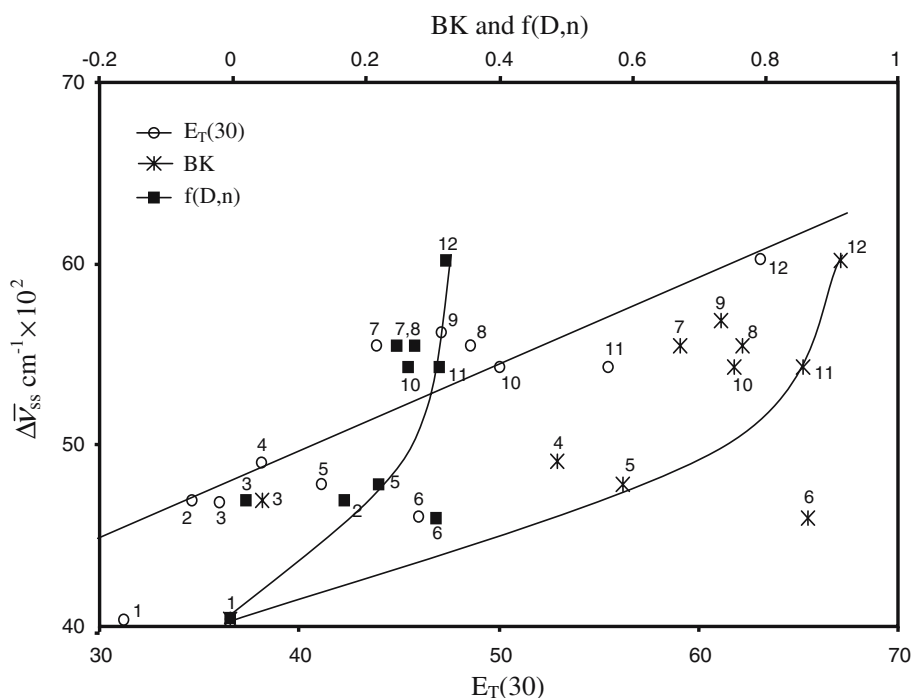


Figure 1. Plot of Stokes shifts ( $\text{cm}^{-1}$ ) of *pABA* versus  $E_T(30)$ , BK and  $f(D,n)$  solvent parameters: 1. cyclohexane, 2. diethyl ether, 3. dioxane, 4. ethyl acetate, 5.  $\text{CH}_2\text{Cl}_2$ , 6.  $\text{CH}_3\text{CN}$ , 7. *t*-butyl alcohol, 8. 2-propanol, 9. 2-butanol, 10. 1-butanol, 11. methanol, 12. water.

Table 1. Absorption,  $\log \epsilon$ , fluorescence spectral data (nm) and Stokes shift ( $\text{cm}^{-1}$ ) of *pABA* in selected solvents

S. no.	Solvents	$\lambda_{\text{abs}}$	$\log \epsilon$	$\lambda_{\text{flu}}$	Stokes shift
1.	Cyclohexane	283.5	3.48	320	4023
		217.0	3.60		
2.	1,4-Dioxane	283.5	3.78	327	4692
		284.0	3.77		
3.	Ethyl acetate	284.0	3.77	330	4908
		219.5	3.71		
4.	Acetonitrile	286.5	3.71	330	4601
		219.0	3.71		
5.	<i>t</i> -Butyl alcohol	286.0	3.83	340	5553
		221.0	3.62		
6.	2-Propanol	286.0	3.82	340	5553
		221.2	3.42		
7.	Methanol	287.0	3.71	340	5432
		217.5	3.46		
8.	Water	282.2	3.47	340	6024
		218.4	3.52		

[23, 24]. The increase in the excited state dipole moment value indicates, *pABA* molecule is more polar in the  $S_1$  state.

#### Effect of hydrogen ion concentration

The absorption and emission spectra of *pABA* have been studied in the  $H_0/pH/H_-$  range of  $-5$  to  $16$ . The relevant data are compiled in Table 2. At  $H_0 -5$ , the species present at  $273$  nm is dication of *pABA*, formed by protonation of the carboxyl group, consistent with the results observed by others for the similar protonation [25]. The blue shift observed in the absorption maxima ( $270$  nm) with decrease of hydrogen ion concentration

( $pH \sim 1$ ) suggest the presence of monocation formed by protonating the amino group. A red shift is observed in the absorption ( $282$  nm) shows that the neutral species is formed in the range from  $pH \sim 3$  to  $3.8$ . Further in this  $pH$  range, the absorption maxima resemble the spectra observed in non-aqueous solvents and thus can be assigned to be neutral species. The absorption spectra exhibit a regular blue shift  $282$ – $265$  nm with an increase in the  $pH$   $4$  to  $5.5$  indicates that monoanion is formed. It is well known fact that deprotonation of carboxyl group gives blue shifted absorption and emission maxima [25]. Above  $H_- 14$  a slight red shift ( $273$  nm) compared to monoanion is observed suggesting that dianion is formed by deprotonating the amino group. The spectral shift

Table 2. Different prototropic maxima (absorption and fluorescence) of *p*ABA in aqueous and  $\beta$ -CD medium

Species	Aqueous				$\beta$ -CD			
	$\lambda_{\text{abs}}$	$\lambda_{\text{flu}}$	$\text{p}K_{\text{a}}$	$\text{p}K_{\text{a}}^*$	$\lambda_{\text{abs}}$	$\lambda_{\text{flu}}$	$\text{p}K_{\text{a}}$	$\text{p}K_{\text{a}}^*$
Dication	273.5 227.0	360	> -3.0	1.0	–	–	–	–
Monocation	270.2 226.0	nf	2.4	2.0	260.4 223.4	nf	2.2	2.4
Neutral	282.0 218.4	350	2.5–3.9	4.0–6.0	284.2 214.4	345	3.5–5.0	3.5–8.0
Monoanion	265.4 215.2	340	5.0	6.5	259.6 214.8	340	6.5	7.5
Dianion	273.5	340 410	> 14.0	> 13.0	–	–	–	–

nf – non-fluorescent.

observed in the last step is similar to what is normally observed in the deprotonation of an amino group [15].

In the  $S_1$  state, when the acidity is increased from pH  $\sim 1.5$  to  $H_0 - 2.0$  a red shifted emission maxima is observed is due to formation of dication in carboxyl group. With the decrease in pH from 4, the emission maxima at 350 nm is quenched because monocation is formed in the amino group. At small hydrogen ion concentration pH  $\sim 4-6$ , the weakly fluorescent maxima (350 nm) indicates in the pH range neutral species is present. With an increase in pH  $\sim 6-10$ , *p*ABA gives a new blue shifted spectra with the maxima 340 nm suggesting the formation of monoanion. Further increase in pH from 13, a large red shift emission maxima (410 nm) is observed could be due to the formation of the  $\text{NH}^-$  ions (dianion). The  $\text{p}K_{\text{a}}^*$  value of neutral-monoanion equilibrium is greater than that in the ground state  $\text{p}K_{\text{a}}$  value. The tendency for carbonyl and carboxyl aromatic compounds to become more basic in the  $S_1$  state relative to the  $S_0$  state is well established [25].

#### Studies of *p*ABA with $\beta$ -CD

The absorption and emission maxima of *p*ABA ( $1 \times 10^{-5}$  mol  $\text{dm}^{-3}$ ) in pH  $\sim 1.0$  and pH  $\sim 7.0$  solutions containing different concentrations of  $\beta$ -CD were also analysed. At pH  $\sim 7$ , *p*ABA exists as a carboxylic anion, hence we also recorded spectrum at pH  $\sim 1$ . The absorption peaks of *p*ABA in pH  $\sim 1$  (monocation) appears at 270 nm and pH  $\sim 7$  (monoanion) absorption peaks appears around 285 nm. In both cases, no clear isosbestic point is observed in the absorption spectra. In the presence of  $\beta$ -CD, there is a slight blue shift (271–269 nm) is observed in the maxima at pH  $\sim 1$ , whereas the absorption spectra of *p*ABA in pH  $\sim 7$  is seen to undergo a marginal red shift (266–284 nm). It has also been observed that both absorption intensities increases with increasing concentration of  $\beta$ -CD. At pH  $\sim 1$ , the absorption spectra does not show any marginal change in absorption maxima even in the presence of the highest concentration of  $\beta$ -CD used ( $1.2 \times 10^{-2}$  mol  $\text{dm}^{-3}$ ). The association constant for the *p*ABA: $\beta$ -CD complex for-

mation has been determined by using Benesi and Hildebrand [26] equation indicates 1:1 complex formed between *p*ABA and  $\beta$ -CD. A plot of  $1/[A-A_0]$  versus  $1/[\beta\text{-CD}]_0$  gives a straight line as shown in Figure 2. From the intercept and slope values of this plot,  $K$  is evaluated. The formation constants for protonated *p*ABA (pH  $\sim 1$ ,  $89 \text{ M}^{-1}$ ) is considerably greater than those of its anionic form (pH  $\sim 7$ ,  $33 \text{ M}^{-1}$ ). The formation constants are very sensitive to change of pH values, which reveals that selective inclusion associated with the species form of *p*ABA. Of the two species of *p*ABA, we should note that,  $\beta$ -CD can readily include the protonated species than the anionic species, because the former is more hydrophobic than the latter. By assuming this orientation for the *p*ABA molecule in the  $\beta$ -CD cavity is easy, because the cyclodextrin cavity favors the neutral form of the benzoic acid derivatives [2, 17]. The higher formation constants in pH  $\sim 1$  implies that the COOH group is more easily embedded in the  $\beta$ -CD cavity than the  $\text{COO}^-$  group of *p*ABA. Further a blue shift at pH  $\sim 1$  suggest, carboxyl group present in the interior of the  $\beta$ -CD cavity, whereas amino group present in the hydrophilic (upper) part of the  $\beta$ -CD cavity. It is well known that substituents of aromatic rings capable of H-bonding can bind the OH groups of the  $\beta$ -CD edges. The energy involved in such H-bond interactions is responsible for the higher binding constants found, when compared to those of the unsubstituted molecule. This pattern in the binding has been detected in the complexes between benzene derivatives and  $\beta$ -CD. Thus, benzene [27] has a formation constant of  $107 \text{ M}^{-1}$ , whereas that for benzoic acid [27] ranges between 126 and  $600 \text{ M}^{-1}$ . This seems to be the case for *p*ABA in pH  $\sim 7$ : the acid will be “anchored” to the  $\beta$ -CD by the  $\text{COO}^-$  group, a factor that confers stability to the complex.

The fluorescence characteristics of *p*ABA in  $\beta$ -CD solutions at pH  $\sim 1$  is different from pH  $\sim 7$  solutions (Figure 3). There is no significant change is observed in emission maxima (350 nm) at pH  $\sim 1$ , but it is red shifted in pH  $\sim 7$  (340–347 nm) with increasing the  $\beta$ -CD concentrations. The emission intensity of *p*ABA

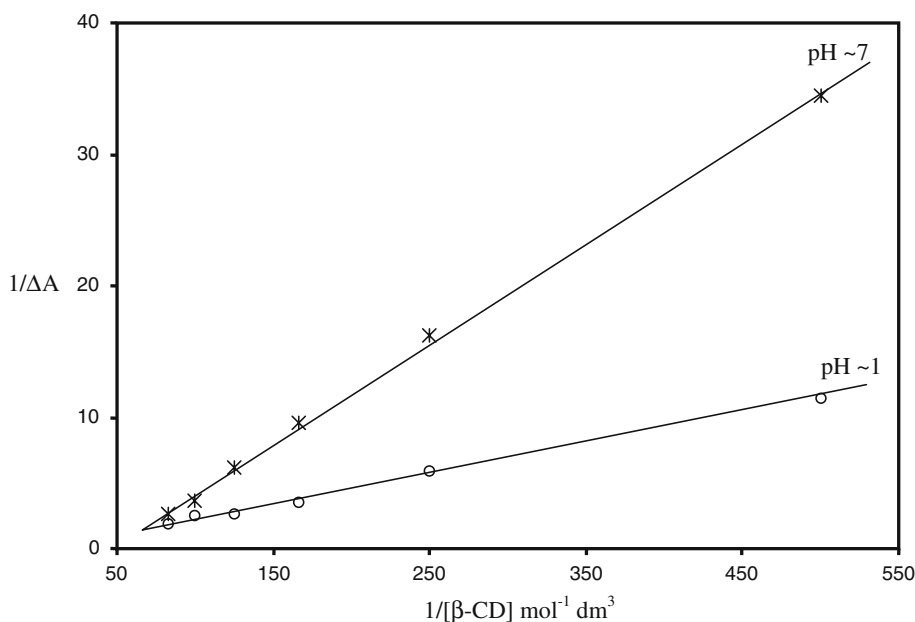


Figure 2. Plot of  $1/\Delta A$  versus  $1/[\beta\text{-CD}]$  for *pABA*.

in pH  $\sim 7$  is decreases when the  $\beta\text{-CD}$  concentration is increased, whereas at pH  $\sim 1$  the fluorescence intensity is increased. The spectral red shifts of *pABA* emission at pH  $\sim 7$  in  $\beta\text{-CD}$  suggest that, COOH group is located within the non-polar cavity of the  $\beta\text{-CD}$  and  $\text{NH}_2$  group is interact with  $\beta\text{-CD-OH}$  groups. This conclusion is based on the following reasons: the large rim of  $\beta\text{-CD}$  contains 12 secondary hydroxyl groups and thus provides an environment qualitatively similar to polyhydroxyl alcohols. The red shift observed (at pH  $\sim 7$ ) in the emission spectrum of *pABA* in  $\beta\text{-CD}$  is consistent with protic solvents. The blue shift observed at pH  $\sim 1$  (absorption) in  $\beta\text{-CD}$  medium is clearly establish that carboxyl group is deeply entrapped in the  $\beta\text{-CD}$  cavity. Since the dipole-dipole interactions between the  $\beta\text{-CD}$  and the carboxyl group is lowered in the less polar environment, (hydrophobic part) a blue shift is observed in pH  $\sim 1$  solutions. Figure 4 shows the Benesi-Hildebrand plot of observed changes in the fluorescence intensity with increasing concentration of  $\beta\text{-CD}$ . It is seen from this plot, that the emission intensity of *pABA* (in pH  $\sim 7$ ) initially decreases with  $\beta\text{-CD}$  concentration and then saturates to a limiting value at  $1 \times 10^{-2}$  M,  $\beta\text{-CD}$ , indicating the incorporation of almost all the *pABA* molecules in the  $\beta\text{-CD}$  cavity.

The difference in spectral change of *pABA* with addition of  $\beta\text{-CD}$  in pH  $\sim 1$  compared to pH  $\sim 7$  suggests that the structural geometry of (*pABA*: $\beta\text{-CD}$ ) inclusion complexes are different in terms of orientation of guest molecule [1, 2]. It is well known, in  $\beta\text{-CD}$  solution hydrophobicity is the driving force for encapsulation of the molecule inside the cavity and naturally the hydrophobic part (COOH) would like to go inside the deep core of the non-polar cavity and the amino group will be the hydrophilic part of the  $\beta\text{-CD}$  cavity. This is reasonable, because at pH  $\sim 7$ , amino group is more polar and can form hydrogen bonds with either  $\text{-OH}$  groups

of the  $\beta\text{-CD}$  cavity rim or bulk water molecules or both. Further, determination of the  $\text{p}K_a$  value of *pABA* indicates that increase/decreases in monoanion/monocation respectively in the presence of  $\beta\text{-CD}$ . This result must mean that amino and COOH groups of the *pABA* molecule completely included in the cavity of  $\beta\text{-CD}$ , otherwise the  $\text{p}K_a$  value of monocation or monoanion should not be altered.

To know the effect of  $\beta\text{-CD}$  on the prototropic equilibrium between monocation, neutral, monoanion on the pH dependent changes in the absorption and emission spectra of the *pABA* molecule in aqueous solution containing  $\beta\text{-CD}$  have been recorded and are shown in Table 2. The absorption and emission maxima of *pABA* have been studied in  $6 \times 10^{-3}$  M  $\beta\text{-CD}$  solutions in the pH range 0.1 to 11. No noticeable change is observed in the absorption maxima of neutral whereas a blue shift is observed in monocation and monoanion of *pABA* in  $\beta\text{-CD}$  medium than aqueous medium. However in the  $S_1$  state, a slight blue shift is observed in neutral maxima, whereas the change in emission maxima of monoanion is negligible (monocation is non-fluorescent). This behavior is different from its ground state, because in the  $S_1$  state, amino group becomes more acidic, whereas COOH group becomes more basic. The  $\text{p}K_a$  ( $\text{p}K_a^*$ ) values of the monocation-neutral equilibrium of *pABA* in  $\beta\text{-CD}$  is lower than aqueous medium, whereas neutral-monoanion equilibrium  $\text{p}K_a$  ( $\text{p}K_a^*$ ) values is greater than aqueous medium. These findings indicates *pABA* is encapsulated in the  $\beta\text{-CD}$  cavity.

This is further supported by using semiempirical quantum calculations MOPAC [28]. This program helped us to draw the structure of the inclusion complex. The ground state geometry of *pABA* and  $\beta\text{-CD}$  were optimized using AM1 method (MOPAC 6/PC). As suggested and found by others [29] this method provides

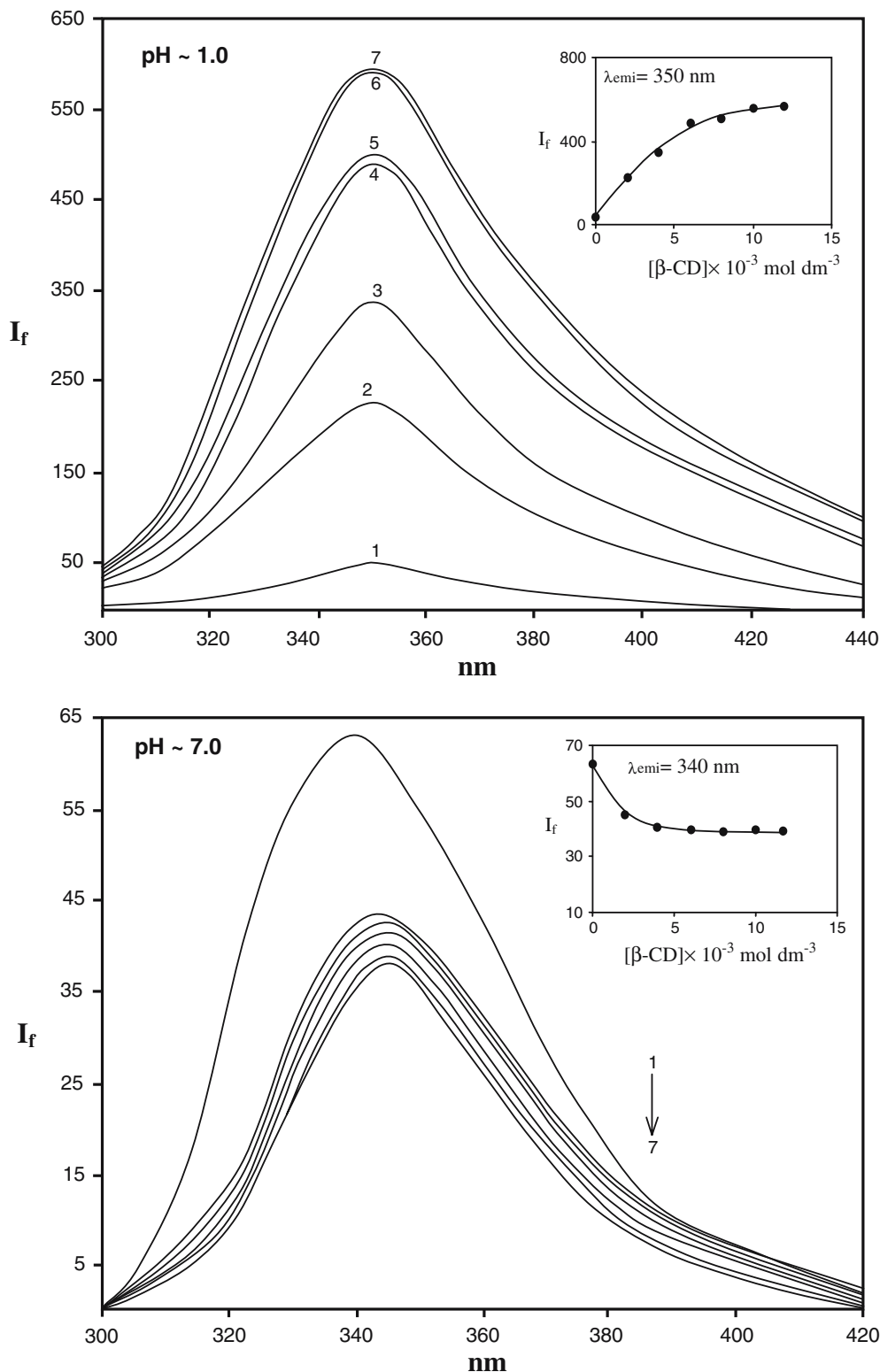


Figure 3. Fluorescence spectra of *p*ABA in different  $\beta$ -CD concentrations ( $\text{mol dm}^{-3}$ ): 1. 0, 2. 0.002, 3. 0.004, 4. 0.006, 5. 0.008, 6. 0.010, 7. 0.012.

acceptable approximations to give results, which are quite close to the experimental finding. The internal diameter of the  $\beta$ -CD is approximately 6.8 Å and its height is 7.8 Å. Considering the shape and dimensions of  $\beta$ -CD, *p*ABA can be completely encapsulated within the  $\beta$ -CD cavity (Scheme 1). Because the distance between

$\text{H}_8\text{-H}_9$  is 7.73 Å and  $\text{O}_1\text{-H}_{10}$  is 6.90 Å and  $\text{O}_2\text{-H}_9$  is 6.77 Å, these values are less than the inside  $\beta$ -CD cavity value. Since the length of *p*ABA is lower than that of the upper/lower rim of  $\beta$ -CD, the amino and carboxylic groups attached to the benzene ring may be present inside the  $\beta$ -CD cavity. The blue shift in the absorption, fluores-

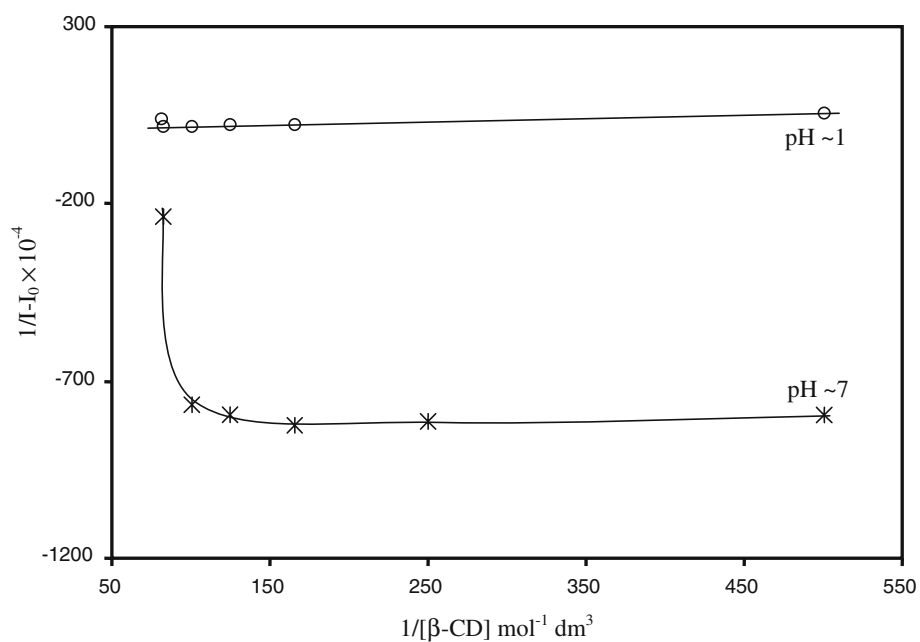
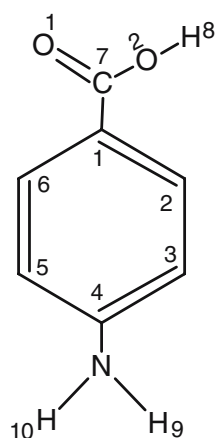
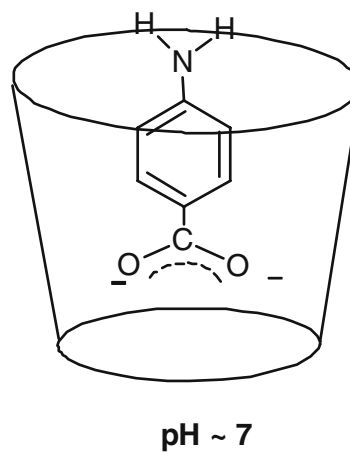
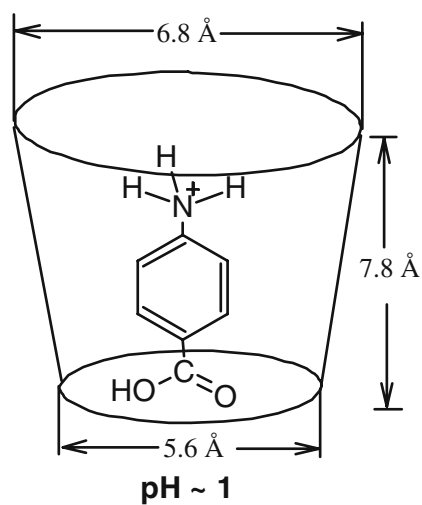


Figure 4. Benesi-Hildebrand plot for the complexation of *p*ABA with  $\beta$ -CD (Plot of  $1/I - I_0$  versus  $1/[\beta\text{-CD}]$ ).



***p*ABA bond distance in**

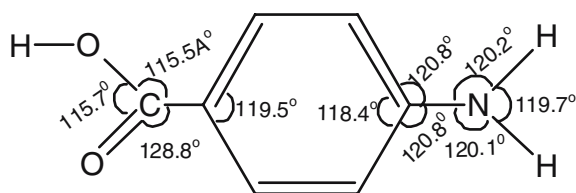
$H_8 - H_9$	=	7.73
$H_1 - H_6$	=	4.32
$O_1 - H_{10}$	=	6.90
$O_1 - H_8$	=	2.23
$H_8 - H_{10}$	=	7.96
$O_2 - H_9$	=	6.77
$O_1 - O_2$	=	2.21



**Inclusion complex**

Scheme 1. Bond distance ( $\text{\AA}$ ) of *p*ABA and  $\beta$ -CD (AM1 method).





cence and FTIR spectra substantiate this. Similar results are also observed in *o*ABA, *m*ABA, syringic acid and naphthols [30].

#### Thermodynamic parameters

There are three important thermodynamic parameters in the inclusion process. The free energy change can be calculated from the formation constant ( $K$ ). The thermodynamic parameters  $\Delta G$ ,  $\Delta H$  and  $\Delta S$  for the association of the guest molecule to  $\beta$ -CD is given in Table 3. As can be seen from Table 3,  $\Delta G$  is negative which suggests that the inclusion process proceeded simultaneously at 303 K.  $\Delta H$  and  $\Delta S$  are also negative in the experimental temperature range which indicates that the inclusion process was an exothermic and enthalpy controlled process. The negative enthalpy change arose from the van der Waal's interaction, while the negative entropy change was the steric barrier caused by molecular geometrical shape and the limit of  $\beta$ -CD cavity to the freedom of shift and rotation of guest molecule.

#### $^1\text{H}$ NMR spectral studies

In order to obtain evidence in support of the structure of the  $\beta$ -CD inclusion complexes with *p*ABA, we measured  $^1\text{H}$  NMR spectra of these *p*ABA molecules with and without  $\beta$ -CD. Owing to the poor solubility of the

Table 3. Binding constant and thermodynamic parameter values of *p*ABA in  $\beta$ -CD medium

Parameters	pH $\sim$ 1		pH $\sim$ 7.0	
	$\lambda_{\text{max}}$	$\lambda_{\text{flu}}$	$\lambda_{\text{max}}$	$\lambda_{\text{flu}}$
$K$ ( $\text{M}^{-1}$ )	89	214	33	232
$\Delta G$ ( $\text{kJ mol}^{-1}$ )	-11.31	-13.51	-8.81	-13.72
$\Delta H$ ( $\text{kJ mol}^{-1}$ )	-70.75		-70.75	
$\Delta S$ ( $\text{J mol}^{-1} \text{K}^{-1}$ )	-0.20	-0.19	-0.20	-0.19.

complex toward  $\text{D}_2\text{O}$ , we are forced to employ at least 8% volume of  $\text{DMSO-}d_6$  as a cosolvent. We define the change in chemical shift ( $\Delta\delta$  ppm) as the difference a chemical shifts between proton signals of the guest or  $\beta$ -CD in the presence and absence of  $\beta$ -CD or the guest. Unfortunately, the addition of 8% volume of  $\text{DMSO-}d_6$  to a  $\text{D}_2\text{O}$  solution of  $\beta$ -CD caused relatively large upfield shifts of the H-3 ( $\Delta\delta = +0.05$ ) and H-5 ( $\Delta\delta = +0.08$ ) signals, allowing us to expect that the presence of this cosolvent lowers the equilibrium constant for the complexation with  $\beta$ -CD and hence, the guest is merely able to induce the small chemical shift of each proton signals for the host.

Chemical shift ( $\delta$ ): *p*ABA (inclusion complex):  $\text{NH}_2 - 4.50$  (4.60)  $\text{H}_2/\text{H}_6 : 7.82$  (7.78);  $\text{H}_3/\text{H}_5 : 6.65$  (6.61). The small upfield shift is observed for  $\text{H}_2$ ,  $\text{H}_3$ ,  $\text{H}_5$  and  $\text{H}_6$  protons suggest *p*ABA included in the  $\beta$ -CD cavity. The downfield shift of the amino protons suggest this protons present in the hydrophilic part of the  $\beta$ -CD cavity. Although, only limited information can be obtained from the  $^1\text{H}$  NMR data, the observation of slight upfield shifts of the guest protons in the presence of  $\beta$ -CD is consistent with the inclusion of each guest into the cavity.

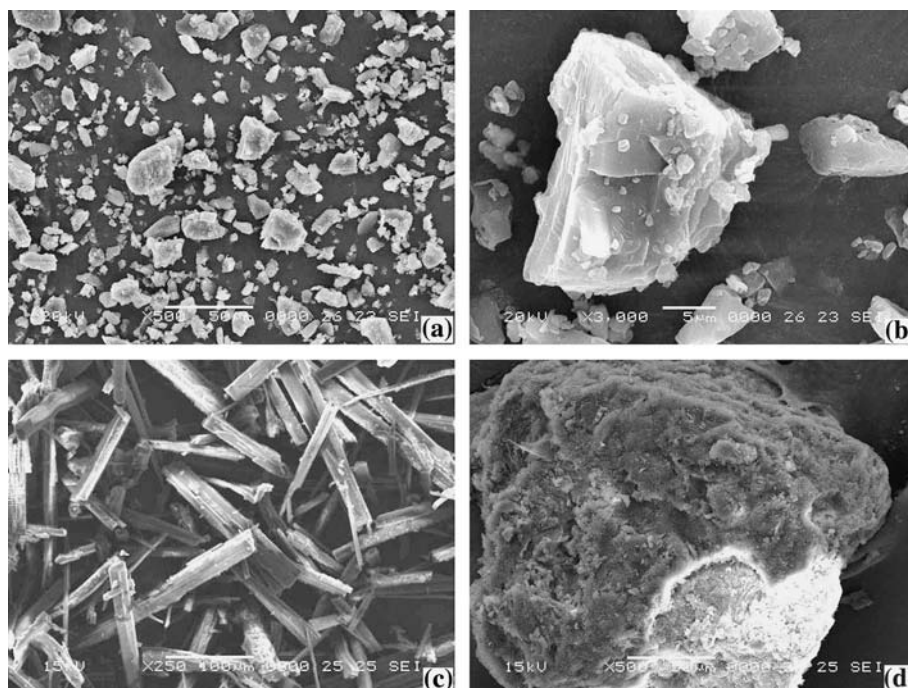


Figure 5. Scanning electron microscope photographs (Pt. coated) of (a)  $\beta$ -CD  $\times$  500, (b)  $\beta$ -CD  $\times$  3000, (c) *p*ABA  $\times$  250 and (d) *p*ABA- $\beta$ -CD complex.



### Microscopic morphological observation

First we observed powdered form of *p*ABA and  $\beta$ -CD by SEM, then we also observed powdered form of inclusion complex (Figure 5). As seen from the SEM figure, (i) pure  $\beta$ -CD is in platted form, (ii) *p*ABA is present in perfect needle structure, and (iii) inclusion complex is present in colloidal structure. This pictures clearly elucidated the difference of powder of each other. Modification of crystals and powder can be assumed as a proof of the formation of new inclusion complex.

### Conclusion

The following conclusions can be drawn from the above studies: (i) solvent studies suggest, ICT interaction in *p*ABA is less than *o*ABA and *m*ABA, (ii) *p*ABA forms 1:1 complex with  $\beta$ -CD, (iii) proton transfer reactions in  $\beta$ -CD medium indicates COOH group present in the hydrophobic part, whereas amino group interact with  $\beta$ -CD –OH groups, (iv) the thermodynamic parameter values shows the inclusion process are exothermic and spontaneous and (v)  $^1\text{H}$  NMR and SEM results confirm *p*ABA form a stable inclusion complex with  $\beta$ -CD.

### Acknowledgements

One of the author (N.R) is thankful to the Department of Science and Technology, New Delhi, for the financial support to the Project under Fast Track Proposal – Young Scientist Scheme No. SR/FTP/CS–14/2005.

### References

1. Y.B. Jiang: *J. Photochem. Photobiol. A: Chem.* **88**, 109 (1995); *Appl. Spectroscopy* **48**, 1169 (1994).
2. S. Shaomin, Y. Yu, and P. Jinghao: *Anal. Chim. Acta* **458**, 305 (2002).
3. (a) Y.H. Kim, D.W. Cho and M. Yoon: *J. Phys. Chem.* **100**, 15670 (1996); (b) Y. Kim *et al.*: *J. Photochem. Photobiol. A: Chem.* **138** (2001) 167.
4. T.C. Schmidt *et al.*: *J. Anal. Chem.* **357**, 121 (1997).
5. T. Vo-Dinh: *Room Temperature Phosphorimetry for Chemical Analysis*, Wiley, New York (1983), pp. 243.
6. S. Panadero, A.G. Hens, and D.P. Bendito: *Talanta* **45**, 829 (1998).
7. R.J. Hurtubise and S.M. Ramasamy: *Appl. Spectroscopy* **45**, 1126 (1991).
8. K. Tatsuya, K. Keisuke, and W. Yutdka: *Anal. Chim. Acta* **367**, 33 (1998).
9. R.M.A. Von Wandruska and R.J. Hurtubise: *Anal. Chem.* **49**, 2164 (1977).
10. R.J. Hurtubise and S.M. Ramasamy: *Anal. Chem.* **59**, 2144 (1987).
11. R.J. Hurtubise, S.M. Ramasamy, J.B. Goates, and R. Putnam: *J. Luminol.* **68**, 55 (1996).
12. (a) A. Nag, T. Chakraborty and N. Chattopadhyay: *J. Photochem. Photobiol. A: Chem.* **52**, 199 (1990); (b) P. Bortulos and S. Monti: *J. Phys. Chem.* **91**, 5046 (1987).
13. A. Nag and K. Battacharya: *Chem. Phys. Lett.* **157**, 83 (1989); *J. Chem. Soc. Faraday Trans.* **86**, 53 (1990); *J. Phys. Chem.* **94**, 4203 (1990).
14. H. Shizuka and M. Hoshino *et al.*: *J. Phys. Chem.* **86**, 4422 (1982); *Bull. Chem. Soc. Jpn.* **58**, 2107 (1985).
15. N. Rajendiran and M. Swaminathan: *J. Photochem. Photobiol. A: Chem.* **93**, 103 (1996); *Bull. Chem. Soc. Jpn.* **68**, 2797 (1995); *Ind. J. Chem.* **40A**, 331 (2001).
16. (a) R. Anithadevi and N. Rajendiran: *Spectrochim. Acta* **61A** 2495 (2005); (b) T. Stalin and N. Rajendiran: *Spectrochim. Acta* **61A** (2005) in press; (c) K. Sivakumar and N. Rajendiran: *Spectrochim. Acta* **61A** (2005) in press.
17. (a) T. Stalin and N. Rajendiran: *J. Photochem. Photobiol. A: Chem.* (in press); (b) T. Stalin and N. Rajendiran: *Chem. Phys.* (in press).
18. M.J. Jorgenson and D.R. Harter: *J. Am. Chem. Soc.* **85**, 878 (1963).
19. G. Yagil: *J. Phys. Chem.* **71**, 1034 (1967).
20. E.A. Steek and G.W. Ewing: *J. Am. Chem. Soc.*, 3397 (1948).
21. C. Reichardt, K. Dimroth, and Forstsch: *Chem. Forsch.* **11**, 1 (1968).
22. L. Bilot and A. Kawski: *Z. Naturforsch.* **18A**, 621 (1962).
23. E. Lippert: *Z. Natureforsch, Teil. A* **17**, 621 (1962).
24. N. Matagai *et al.*: *Bull. Chem. Soc. Jpn.* **28**, 690 (1955).
25. (a) J.K. Dey, S.K. Dogra: *J. Photochem. Photobiol. A: Chem.* **59**, 307 (1991); (b) H.K. Sinha and S.K. Dogra: *Spectrochim. Acta* **45A**, 1289 (1989).
26. H.A. Benesi, and J.H. Hildebrand: *J. Am. Chem. Soc.* **71**, 2703 (1949).
27. (a) A. Sytniz and C.D. Valle: *J. Phys. Chem.* **99**, 13028 (1995); (b) G.G. Gaitano *et al.*: *J. Phys. Chem.* **108A**, 392 (2004).
28. M.J.S. Dewar *et al.*: *J. Am. Chem. Soc.* **107**, 3902 (1985).
29. (a) S.K. Das, *Chem. Phys. Lett.* **361**, 21 (2002); (b) S. Panja and S. Chakravorti, *Chem. Phys. Lett.* **336**, 57 (2001).
30. R.A. Agberia, R. Uzar, and D. Gill: *J. Phys. Chem.* **93**, 3855 (1989).